Extraction of Pressure Features for Predicting Driver Posture

Mingming Zhao, Georges Beurier, Hongyan Wang, Xuguang Wang*

Abstract Postural information of drivers is helpful for specifying take-over control as well as for developing intelligent protection systems in autonomous vehicles. Thanks to the ease of use and the robust performance under varying environments, a pressure sensor could be a good alternative or complementary to cameras for monitoring drivers' postures, especially for the trunk and feet. However, association between pressure distribution and posture is still unclear, effective methods for postural classification from pressure measurement therefore need to be developed.

The objective of this study was to propose a method for extracting relevant features from the original pressure distribution data to predict drivers' posture. First, a large number of pressure parameters, including contact area proportions, centres of pressure and pressure ratios, were defined for generating pressure features and the relevancy was analysed by performing the Out-Of-Bag feature importance evaluation of a Random Forest classifier. Finally, the relative value changes of 15 important parameters were used as features for training the classifier, leading to an average accuracy of 77.4% across nine posture classes and 23 drivers in the Leave-One-Out cross-validation tests. This study will provide valuable insight for extracting features in order to develop robust postural monitoring systems using pressure measurement.

Keywords Driver posture monitoring, driving safety, machine learning, pressure features

I. INTRODUCTION

Over 1.35 million fatalities and more than 50 million serious injuries worldwide each year are claimed by road traffic accidents [1], most of which have been reportedly attributed to human errors in recognition, decision and performance [2]. Driving automation has great potential of accommodating human errors, but also gives rise to new types of safety concerns. One critical issue concerns the transition between the human driver manoeuvres and automated operations. For the autonomous vehicles of Level 3 (SAE), human drivers are required to stay within the control loop, it is imperative to monitor drivers' behaviour to evaluate his/her intention and readiness for a safe transition [3]. Another consistently mentioned topic is the passive safety in autonomous vehicles. With the increased diversity of in-vehicle activities and the innovation of seating arrangements [4], drivers may adopt other seated postures than the conventional driving position. Existing restraint systems may not provide efficient protection for these new postures in case of accidents. To reduce the injury risk, a possible solution could be the development of an intelligent system that can adjust the seat configuration prior to collision [5] and modulate the response of the restraint system during collision [6], based on the real-time tracking of driver posture.

Driver posture can be monitored by means of different methods [7], such as computer vision or pressure measurement based systems, among many others. Being able to provide visual details, cameras are playing a predominant role in this domain. However, the performance of camera-based

Xuguang Wang (xuguang.wang@ifsttar.fr, +33 4 72142451) is a Research Director of Université Gustave Eiffel at the Laboratory of Biomechanics and Impact Mechanics, France. M. Zhao (mingming.zhao@ifsttar.fr) is a joint training PhD student in Biomechanics at Université Claude Bernard Lyon 1 (UCBL1), France and Tongji University, Shanghai, China. G. Beurier is a Researcher at the Laboratory of Biomechanics and Impact Mechanics, a mixed research unit of UCBL1 and Université Gustave Eiffel (formerly known as IFSTTAR), France. H. Wang is a Professor of Vehicle Engineering in the School of Automotive Studies at Tongji University in Shanghai.

monitoring systems is subject to lighting condition, camera placement in the cabin and the occurrence of body occlusions in the field of view. In contrast, pressure sensors can be unobtrusively integrated into a seat and do not suffer from the limitations exhibited by cameras. Pressure sensor could be a good alternative or complementary to optical vision systems, i.e., cameras, for monitoring driver postures, especially for the trunk and feet.

In recent years, there has been growing interest in using pressure measurement as an approach for driver monitoring. Reference [8] used a Support Vector Machine (SVM) classifier which was trained directly by the raw pressure measurements on both backrest and seat pan collected from a driving simulator to classify eight driver activities (pressing accelerator, looking right/left, looking right/left rear, holding phone right/left and pressing brake). Seven drivers participated in the experiment and a total estimation error of 41% was found for the test data randomly selected from all the participants. The authors also performed an on-road experiment to detect only feet behaviours for predicting pedal engagement using the same method. An average estimation error of 7.55% has been claimed. However, in both cases, they did not test the classifier on a new driver whose data was not used for training. Reference [9] also used the SVM technique. Apart from the original pressure measurement from backrest and seat pan, the authors added the changes of the Centre of Pressure (COPs) with respect to their normal positions as explanatory variables to distinguish three activities including cell phone use, forward gaze (normal state) and sleeping performed by 14 drivers. An accuracy of 76.8% by the Leave-One-Out (LOO) cross-validation for new drivers was achieved. In both studies [8-9], the authors intended to predict predefined driver postures directly from the pressure measurement, without explicitly specifying the driver trunk positions. As pressure results from the contact between the trunk and thighs with the seat, activities mainly involving the movement of head or hands without trunk movement are difficult to be detected. This may explain why a low classification accuracy was obtained by the both studies (i.e., 15% and 20% were determined for looking right/left in [8] and 59.6% for the forward gaze in [9]). In [10], an array of force sensors were deployed to detect if a driver was in Out-Of-Position (OOP). To consider the inertia effect by vehicle dynamics, an accelerometer was implemented to monitor the vehicle acceleration. By analysing the COP trajectories and vehicle acceleration, three types of OOP (forward, left and right inclined trunk positions) could be detected. However, the system was not evaluated quantitatively.

In our earlier study [11], nine classes of in-vehicle postures from 23 drivers were identified by analysing the trunk and feet positions. In contrast to other studies [8-10], our posture classes covered a wider range of driver postures that a driver can adopt when driving or performing non-driving tasks. A deep learning classifier was trained on the pressure distribution images to detect these postures. An average classification accuracy of up to 94% was obtained for a driver whose data was used for training the classifier. The same classifier was also used to continuously predict postural changes during a motion. By tracking the class score changes, driver postural change could be correctly predicted. For the LOO cross validation tests, however, the classification accuracy dropped to 51% on average and the continuous prediction also suffered. One reason may be that pressure distribution changes due to inter-individual variability (e.g., body size, seating preference) were not separated enough from those by postural change. Essentially, the continuous prediction depended on the classification accuracy. Therefore, a reliable classifier plays a key role in predicting driver postural changes. Although advanced methodologies such as deep learning models are able to automatically extract high-level features from the raw input images, each problem is domain specific and the model generalisation can be improved by transforming raw data into features that better represent the underlying problem [12]. In our preliminary study [13], a few pressure parameters such as the pressure ratios between regional contact areas were investigated and the results showed that the movement of trunk and feet could possibly be described by analysing the pressure parameter changes. Therefore, in order to develop a more robust pressure sensor based postural monitoring system, pressure parameters that are more relevant to characterise body movement need to be identified.

The aim of the current study was to extract features from relevant pressure parameters to predict drivers' postural change using a machine learning classifier. The classifier trained on these features is expected to be better than the one trained on raw pressure data in terms of generalisation capability. First, we systematically constructed a set of parameters from the original pressure distribution data. Secondly, the relevance of these parameters was evaluated using a Random Forest model. Finally, posture classification performance based on the selected features was evaluated.

II. METHODS

Experiment

Twenty-three volunteers (11 females and 12 males) with at least three years of driving experience participated in the experiment. They varied in age from 22 to 65 years (M=40, SD=11.5), in height from 153 to 195 cm (mean=171, SD=13) and in Body Mass Index (BMI) from 18.2 to 43.4 kg/m2 (mean=27.8, SD=6.7). Participants provided written informed consent prior to the experiment. Université Gustave Eiffel (formerly IFSTTAR, French Institute of Science and Technology for Transport, Development and Networks) Ethics Committee approved the experimental protocol.

To ensure good coverage of in-vehicle driver postures, 42 driving and non-driving activities defined from a related study [14] were adopted. They consisted of primary driving operations such as standard driving, braking, switching gear, etc., secondary driving activities such as controlling the navigation system, picking up something in the car, etc., as well as possible new actions that may occur in an autonomous vehicle such as relaxing with both feet on the floor, holding a book with both hands, etc. For each task, the standard driving posture (with two hands on the steering wheel, trunk in normal position, left foot on floor and right foot on acceleration pedal) served as both the starting and end postures.

During the experiment, participants were instructed to perform these tasks in a random order on a mock-up simulating the interior of an existing vehicle (Fig. **1**). Pressures on the seat pan and backrest contact surfaces were measured by two Xsensor pressure mats (Model: PX 100: 48.48.02) with a sampling frequency of 25 Hz. Body positions during a motion were recorded by a marker-based optical motion capture system VICON with a frequency of 50 Hz. In addition, movements were also recorded by a Kinect sensor for further visual cross-reference. All the measurement systems were synchronised by using a common electronic trigger.

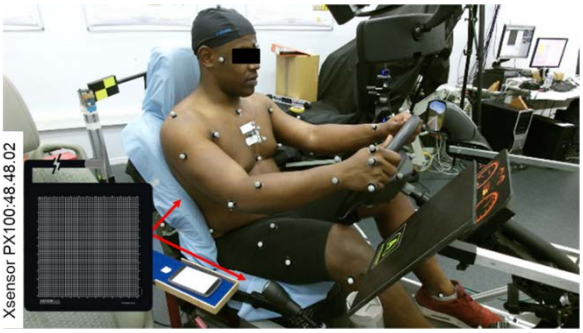

Fig. 1. Experimental rig

Definition of In-vehicle Posture Classes

Driver motions recorded by the VICON system were reconstructed using RPx [15], a custom human model based motion analysis and simulation tool. For motion reconstruction, the body was simplified as a skeleton model with 28 articulated joints from head to feet (Fig. 2), and a posture was represented by an array of joint angles or joint positions. As pressure distribution on the seat is not sensitive to the movement of the head and arms, we decided to differentiate driver postures mainly by trunk and feet positions. Global trunk position was characterised by three angles (axial rotation angle, forward inclination angle and lateral tilt angle, see Fig. 2) relative to the normal trunk position in the standard driving posture.

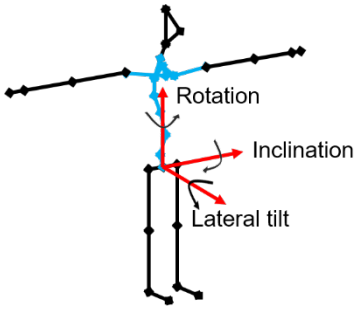

Fig. 2. Driver skeleton model and trunk coordinate system

To define different posture classes for labelling, we first extracted distinctive trunk positions from 3D reconstructed motions. Empirically two ellipsoid envelopes were defined in the trunk angle space (axial rotation, forward inclination and lateral tilt) with half the length of the principal axes being (5°, 3°, 2°) and (30°, 25°, 20°), respectively. The smaller envelope defined the standard driving postures. The intermediate transitional trunk positions between the two envelopes were excluded to avoid label ambiguity. For the trunk positions outside the larger envelope, a cluster analysis using mean shift [16] was performed to group them into six classes. In addition, four feet position classes were also identified. In total, nine posture classes were defined considering the trunk and feet positions.

Pressure Distribution Data Processing

According to the effective contact area between drivers and seat, the original pressure sensing area was tailored to 42 by 44 sensor elements for both seat pan and backrest mats. Raw data was smoothed by an averaging window of 3 by 3. To reduce the pressure variation due to body weight, pressure value was normalised by the peak on each mat. Thanks to the use of the trigger system, the correspondence between the posture class labels and pressure data was established.

Identification of Relevant Pressure Parameters

The pressure parameters relevant for describing postural change were extracted using a four-step process. First, we calculated the pressure standard deviation of each sensor across the standard driving postures performed by all the participants (see Appendix: Fig A1). The higher standard deviation is, the more sensitive to the inter-individual change the corresponding sensor is. Secondly, to gain knowledge about how the pressure distribution changes due to body movement, the pressure standard deviations of each sensor were averaged across all participants performing the same task (see Appendix: Fig A2 for some examples). The higher the standard deviation is, the more sensitive to body movement the corresponding cell is. Thirdly, by inspecting the pressure variation due to inter-individual and postural changes, we segmented the backrest and seat pan pressure mats into 12 (B1-B12) and 8 (S1-S8) sub areas as shown in Fig. 3. Finally, based on the segmentation of the pressure mats, 24 pressure parameters (Appendix: TABLE AI) were constructed by analysing pressure pattern changes. These parameters fell into three categories: Contact Area proportion (CA, the proportion of sensor elements on the pressure mat activated by body contact), Centre of Pressure (COP, 2D position of application of the resultant force in a sensing area) and Pressure Ratio (PR, the ratio between the sums of pressure from different sensing areas.

To illustrate the principle behind the parameter construction process, two examples are shown in Fig. 4. The first one (Fig. 4a) corresponds to the reference posture when the right foot was on the acceleration pedal, while the second (Fig. 4b) corresponds to the posture when the right foot was on braking pedal. Due to the right foot movement, the pressure distribution patterns were very different from the reference, especially in the right part of the seat pan. Thus, we intuitively defined a set of parameters to characterise the pressure pattern change due to postural change. In this case, the COP position of the right front part of seat pan (S6+S8) in medial-lateral direction (COP_SAR_ML), the pressure ratio between the right front part (S6+S8) and the right part of seat pan (PR_SAR_SR), etc.

Similarly, we inspected the pressure pattern changes due to left foot, trunk movement to define relevant parameters (Appendix: TABLE AI).

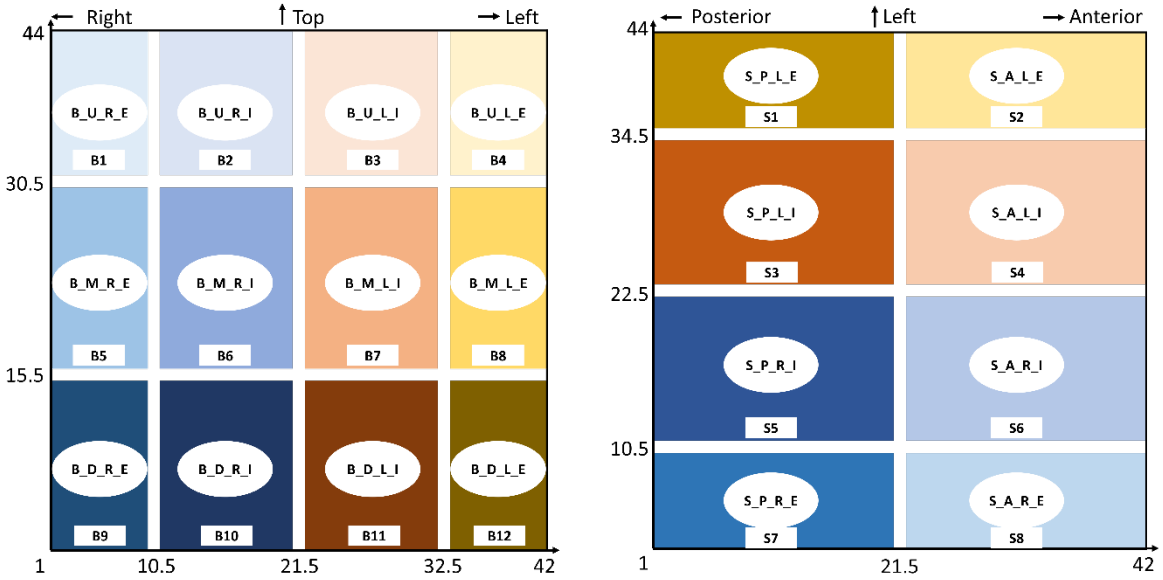

(a) Backrest (b) Seat pan

Fig. 3. Pressure map segmentation. Twelve sensing areas were defined for the backrest mat (a) and eight for the seat pan mat (b). The positions of all boundaries are set empirically. For the convenience of constructing parameters, all sub areas were named using the following convention: [Backrest/Seat pan]_[Up/Middle/Down part of backrest or Posterior/Anterior part of seat pan]_[Left/Right side of backrest or seat pan]_[Exterior/Interior part of backrest or seat pan in medial-lateral direction]. They were also numbered.

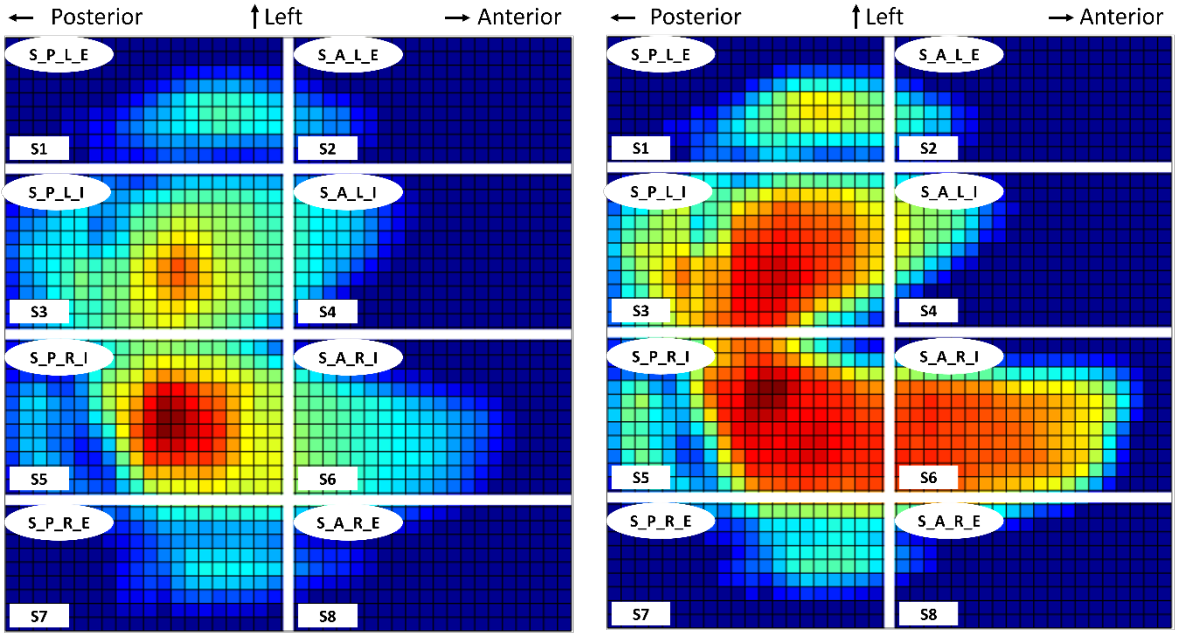

(a) Right foot on acceleration pedal (b) Right foot on brake pedal

Fig. 4. Pressure pattern change on seat pan when driver applied braking.

In addition to the 24 parameters defined by inspecting the change of pressure distribution due to postural change, the sum of the pressure from each of the 20 sub areas was also incorporated. Based on these 44 parameters, two feature vectors were generated. The original feature vector $F_1(t)$ simply

took the current parameter values at frame t of one motion trial. The relative feature vector $F_2(t)$ consisted of the parameter changes at the current frame t relative to their initial value at the beginning of each trial, where drivers had adopted the standard driving posture.

Parameter Selection

The importance of the 44 pressure parameters were evaluated by training a Random Forest (RF) model [17], which is an ensemble of decision trees using the bagging (bootstrap aggregating) technique [18]. During the training process, the model randomly selects a subset of parameters and draws N out of N observations in the data set with replacements for growing each decision tree. The left out observations, approximately one third, are called *Out-Of-Bag (OOB)* observations. These OOB observations were used to evaluate the performance of the RF model. In addition, by randomly permuting OOB observations across one parameter at a time, the increase in the OOB classification error due to this permutation can be estimated. The larger the OOB error is, the more powerful the parameter is for postural classification, thus the more important it is. The importance of a parameter p is quantified by Eq. 1.

$$Importance_p = \bar{d}_p \Big/ \sigma_p \qquad \text{Eq. 1}$$

Where $\bar{d}_p$ and σ_p are the mean and standard deviation of increased OOB error (d_p) for all the decision trees when permuting the parameter p.

The relative feature vector $F_2(t)$ was used to train the RF classifier for evaluating the importance of each parameter. Based upon the results of the feature importance analysis, we evaluated the classifiers trained with a different combination of parameters, starting from the first two most important until all parameters were included by adding a less important one each time.

Validation

Two different sets of RF classifiers were trained for comparison purposes. The first one (RF1) was trained to classify all the nine posture classes using all the parameters from the original feature vector $F_1(t)$, while the second one (RF2) was trained to classify all the nine posture classes using the selected important parameters from the relative feature vector $F_2(t)$. To test the generalisation of the classifiers, a Leave-One-Out (LOO) cross-validation for each participant was performed. For each subject, the data of the other 22 participants was used as training data. For evaluating the classifier's performance, we used $F1\ Score$ to quantify the classification accuracy. $F1\ Score$ is a harmonic mean of Precision (the number of true positive predictions divided by the total number of true positives and false positives) and Recall (the number of true positive predictions divided by the total number of true positives and false positives) of each class. Finally, the best classifier was used to continuously predict the posture changes in a motion.

III. RESULTS

Driver Posture Classes

Six distinctive trunk positions were determined based on the extent to which the trunk deviated from the initial position as shown in Fig. 5a. Four feet positions were extracted from trials where drivers pressed the acceleration pedal, pressed the brake pedal, switched gear and relaxed both feet on the floor (Fig. 5b). Combining the distinctive trunk positions and feet positions gave rise to nine driver posture classes (P0-P8, Fig. 5c) with 5,262 data samples in total. As the postures in P0 were very similar to the initial posture at the beginning of each trial, they were collectively called the standard driving posture.

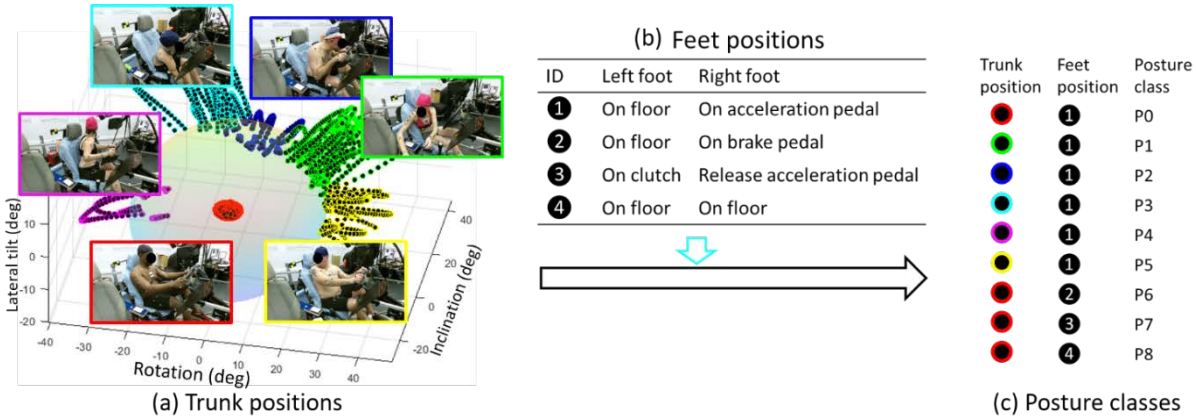

Fig. 5. Typical posture definition scheme. The positive direction of each dimension in (a) denotes right rotation, forward inclination and lateral right tilt.

Parameter Selection

The 44 parameters were ranked in descending order according to their importance (Fig. 6). The mean value was around 2.0. The contact area proportion of backrest (CA_B) had the highest importance (17.1), followed by the pressure ratio between the sub area $B5$ and the whole backrest (PR_BMRE_B) and the pressure ratio between the combined area $B2 + B6 + B10$ and the whole backrest (PR_BRI_B), with a parameter importance of 7.6 and 6.8, respectively. Among the parameters related to the seat pan, the pressure ratio between the sub area $S6$ and the whole seat pan (PR_SARI_S) and the COP of the combined sensing area $S2 + S4$ in medial-lateral direction (COP_SAL_ML) are in the leading positions, with a parameter importance of 3.1 and 2.1, respectively. The lowest value (0.6) was found for the pressure ratio between the sub area $S2$ and the whole seat pan (PR_SALE_S).

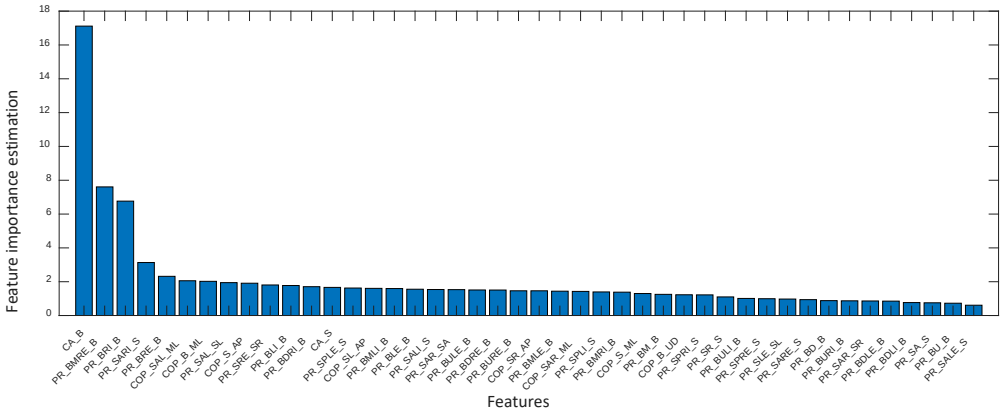

Fig. 6. Parameter importance estimated by RF model

The performance of different RF2 classifiers was shown in Fig. 7. The OOB error decreased rapidly from 38% (when only the first two most important parameters were used to train the model) to 6% (when the first seven most important parameters were used). When more than 15 first parameters were used, the OOB error of the models remained stable around 4.5%.

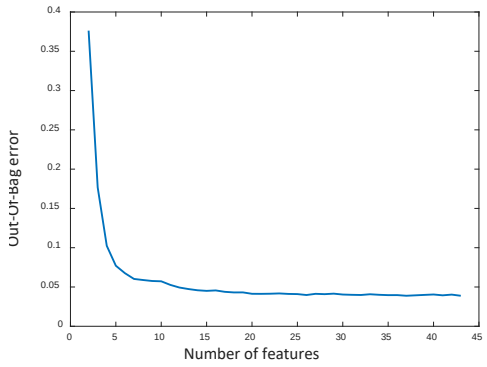

Fig. 7. OOB error vs. number of parameters selected by their importance

Leave-One-Out (LOO) Cross-validation

The first 15 important parameters were used as predictors for training RF2 (using relative feature vector F2). The LOO cross-validation results for these two classifiers are given in TABLE I. Although RF1 was trained with all the features from the original feature vector F1, the $F1\ Score$ of each class was lower than using RF2 which was trained with only the first 15 features from the relative feature vector F2. By a detailed examination of classification errors, we found that P0 and three feet positions (P6-P8) could hardly be distinguishable by RF1. Without considering the feet positions, an accuracy of 97.7% was found for class P0. This classifier is named RF1-6C, also shown in TABLE I. In case the initial posture was known, an average $F1\ Score$ of 77.4% (SD=19.3%) was achieved by RF2. Using RF2, all classes were recognised with an accuracy higher than 74% except for P6 (60.0%, driver pressed brake pedal) and P8 (34.7%, driver relaxed both feet on floor).

TABLE I

LOO CROSS-VALIDATION RESULTS – *F1 SCORE* (N=5262)

Class	P0	P1	P2	P3	P4	P5	P6	P7	P8	Avg	SD
RF1	70.8%	88.1%	32.4%	55.1%	71.5%	76.4%	10.9%	53.6%	11.3%	52.2%	28.2%
RF1-6C	97.7%	88.2%	37.5%	55.4%	75.7%	71.2%	-	-	-	71.0%	21.9%
RF2	78.5%	95.2%	74.2%	84.5%	85.9%	92.3%	60.0%	91.4%	34.7%	77.4%	19.3%

IV. DISCUSSION

The main objective of the present work was to extract features from pressure parameters that are more relevant to characterise the postural change of drivers while less sensitive to inter-individual differences. Four out of the first five important parameters were from backrest, suggesting the importance of backrest pressure mat for postural monitoring. This is in agreement with the fact that the trunk postural change had a higher effect on pressure distribution especially on the backrest. For example, the trunk forward inclination was accompanied by contact area reduction between the backrest and back. Furthermore, feet movement also result in pressure distribution changes on the backrest, as shown in Fig A2 (Appendix). Another point that should be noted here is that 12 of the intuitively defined parameters were found within the first 15 important parameters, suggesting the effectiveness of our intuitive parameter construction process. Trained on the first 15 important parameters, the model could achieve an accuracy of 95.5% for classifying the OOB observations, while models trained on more parameters did not improve their performance.

Using the relative features from the carefully selected 15 parameters, the classifier RF2 performed much better than the classifier RF1 trained with all the 44 original features. This was because the relative features removed the impact of different driver anthropometry and seating preferences on the pressure distribution pattern. However, for practical application, a reference standard driving posture was required to construct the relative feature vector F_2 before using the classifier RF2. To this

end, the normal trunk position could be estimated by the classifier RF1-6C, which provided extremely good recognition of posture P0 (97.7%). The normal feet positions (right foot on acceleration pedal and left foot on floor) could be predicted by analysing the information from integrated pedal sensors.

It should be noted that, relative low accuracy was determined by the classifier RF2 for the postures when braking (P6) and relaxing the feet on the floor (P8). This was due to the individual behavioural differences when performing these tasks. For example, when applying the brakes, some of the drivers just slightly rotated the right calf to reach the brake pedal, while some drivers would first shift the right foot to the left before the pressing action. For relaxing the feet on the floor, the difference between the foot positions of different drivers were also observed. As a result, if the test driver did not perform the tasks in a similar way that was present in the training data, the results would suffer. One solution could be the use of additional pressure sensors implemented on the floor.

The segmentation of the original pressure mat played a key role in identifying relevant pressure parameters. The main purpose of segmentation was to provide access to interpretable pressure parameters that were informative for predicting driver postural changes. In this work, the two pressure mats were segmented into 20 sub areas. An advantage of segmentation was that the original pressure mats were simplified as a combination of 8 or 12 isolated small pressure sensors. Given the expensive price of the pressure sensor, it is tempting to think that a cost-effective solution could be achieved by reducing the number of pressure cells while maintaining the effectiveness of the parameters. This is an interesting topic and will be one of the future research directions.

Another direction of future work is to expand the study to a larger dataset with more postures and more drivers in order to further improve the classifier. In addition, we will perform continuous posture recognition using the classifier, as we did with the deep learning method in [11], to predict driver posture changes in complete motions.

V. CONCLUSIONS

Pressure parameters that are more sensitive to driver postural variation while less affected by inter-individual differences were constructed and selected by a machine-learning algorithm. The prediction model trained with the relative features of 15 important pressure parameters could achieve an average classification accuracy of 77.4% across 9 in-vehicle posture classes and 23 different drivers. Accurate recognition of feet positions using seat pressure mapping alone is still challenging. Adding additional contact sensors on the floor and pedals could be a solution. The method proposed by this study provides valuable insight regarding the selection of meaningful and appropriate pressure features for predicting driver's postures.

VI. ACKNOWLEDGEMENT

This study was funded by China Scholarship Council (CSC 201806260131) and partly supported by the French National Project ANR AutoConduct (ANR-16-CE22-0007).

VII. REFERENCES

[1] World Health Organization. "Global Status Report on Road Safety" Internet https://www.who.int/publications-detail/global-status-report-on-road-safety-2018. [cited 2020 February 20].

[2] Singh, S. Critical Reasons for Crashes Investigated in The National Motor Vehicle Crash Causation Survey. 2015: Washington, DC, USA.

[3] Lu, Z., Happee, R., Cabrall, C.D., Kyriakidis, M., and de Winter, J.C. Human Factors of Transitions in Automated Driving: A General Framework and Literature Survey. Transportation research part F: traffic psychology and behaviour, 2016. 43: p. 183-198.

[4] Jorlöv, S., Bohman, K., and Larsson, A. Seating Positions and Activities in Highly Automated Cars–A Qualitative Study of Future Automated Driving Scenarios. Proceedings of IRCOBI Conference, 2017. Antwerp, Belgium.

[5] Jin, X., Hou, H., Shen, M., Wu, H., and Yang, K.H. Occupant Kinematics and Biomechanics with Rotatable Seat in Autonomous Vehicle Collision: A Preliminary Concept and Strategy. Proceedings of IRCOBI Conference, 2018. Athens, Greece.
[6] Filatov, A., Scanlon, J.M., Bruno, A., Danthurthi, S.S.K., and Fisher, J. Effects of Innovation in Automated Vehicles on Occupant Compartment Designs, Evaluation, and Safety: A Review of Public Marketing, Literature, and Standards. 2019, SAE Technical Paper.
[7] Wang, H., Zhao, M., Beurier, G., and Wang, X. Automobile Driver Posture Monitoring Systems: A Review. China Journal of Highway and Transport, 2019. 32(2): p. 1-18.
[8] Ding, M., Suzuki, T., and Ogasawara, T. Estimation of Driver's Posture Using Pressure Distribution Sensors in Driving Simulator and On-Road Experiment. Proceedings of IEEE International Conference on Cyborg and Bionic Systems (CBS), 2017. Beijing, China.
[9] Okabe, K., Watanuki, K., Kaede, K., and Muramatsu, K. Study on Estimation of Driver's State During Automatic Driving Using Seat Pressure. Proceedings of International Conference on Intelligent Human Systems Integration, 2018. Dubai, United Arab Emirates.
[10] Vergnano, A. and Leali, F. Out of Position Driver Monitoring from Seat Pressure in Dynamic Manoeuvres. Proceedings of International Conference on Intelligent Human Systems Integration, 2019. San Diego, CA, USA.
[11] Zhao, M., Beurier, G., Wang, H., and Wang, X. Driver Posture Prediction Using Pressure Measurement and Deep Learning. Proceedings of IRCOBI Asia Conference, 2020. Beijing, China. (to be published).
[12] Guyon, I., Gunn, S., Nikravesh, M., and Zadeh, L.A., "Feature Extraction: Foundations and Applications", pages 139-165, Springer, Basel, Switzerland, 2008.
[13] Zhao, M., Beurier, G., Wang, H., and Wang, X. Detection of Driver Posture Change by Seat Pressure Measurement (Short communication). Proceedings of IRCOBI Conference, 2019. Florence, Italy.
[14] Dingus, T.A., Klauer, S.G., et al. The 100-car Naturalistic Driving Study, Phase II-Results of The 100-car Field Experiment. 2006: Virginia, Minnesota.
[15] Monnier, G., Renard, F., Chameroy, A., Wang, X., and Trasbot, J.J.S.T. A Motion Simulation Approach Integrated into A Design Engineering Process. SAE Transactions, 2006. (2006): p. 1118-1123.
[16] Comaniciu, D. and Meer, P. Mean shift: A Robust Approach toward Feature Space Analysis. IEEE Transactions on Pattern Analysis & Machine Intelligence, 2002(5): p. 603-619.
[17] Breiman, L. Random Forests. Machine learning, 2001. 45(1): p. 5-32.
[18] Breiman, L. Bagging Predictors. Machine learning, 1996. 24(2): p. 123-140.

VIII. APPENDIX

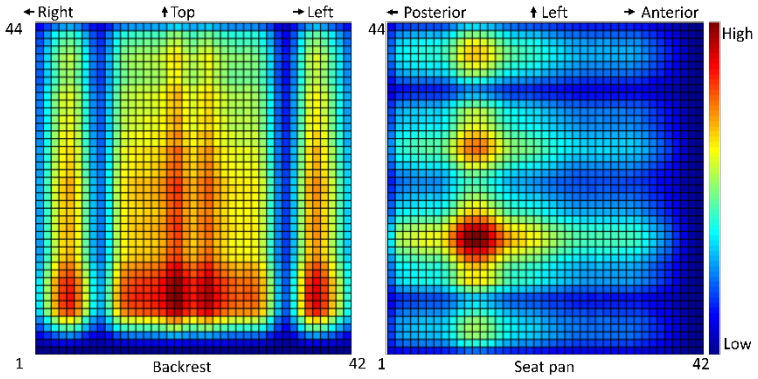

Fig A1. Pressure standard deviation across the standard driving postures of all drivers. The pressure standard deviations were normalised by the corresponding peak of each mat. The inconsistency within the pressure standard deviation maps are mainly caused by the ergonomic design of the driver seat surface. On the seat pan, the pressure in medial-lateral direction is asymmetrically distributed. This is because of the different placements of the feet, i.e., right foot on the throttle while left foot on the floor.

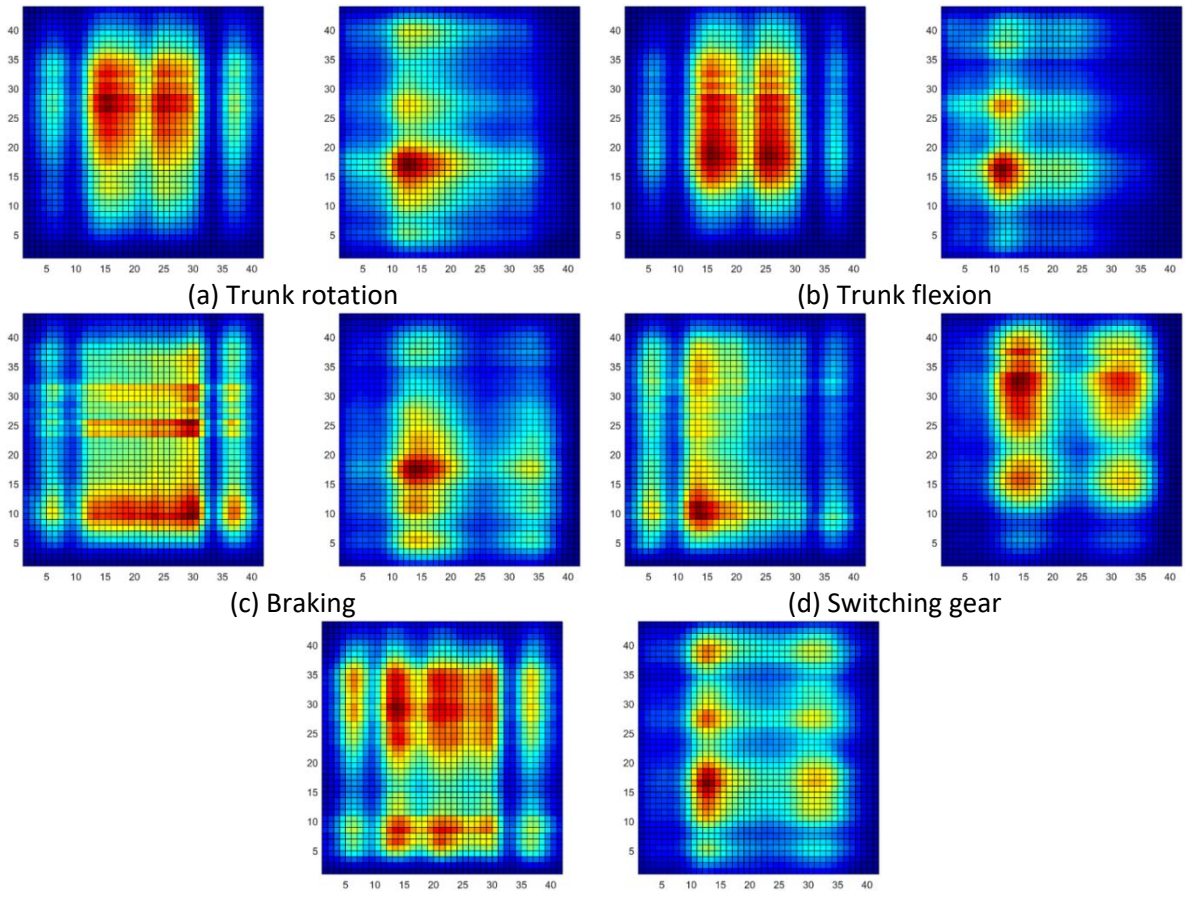

(a) Trunk rotation (b) Trunk flexion

(c) Braking (d) Switching gear

(e) Crossing legs

Fig A2. Pressure standard deviation across body part movement of all drivers (the backrest is on the left and seat pan on the right). The pressure standard deviations were normalised by the corresponding peak of each mat. The pressure changes concentrated on the upper part of the backrest when driver rotates the trunk (a). When driver inclined the trunk in anterior-posterior direction, the pressure changes were mainly located at the middle part of backrest (b). When driver moved the feet, the front part of the seat pan saw remarkable pressure changes, as shown by the

cases in (c), (d) and (e). Another information we could draw from these observations is that any body movement related to trunk or thigh will cause pressure changes on both backrest and seat pan.

TABLE AI

SPECIFICATION OF PRESSURE PARAMETERS FOR EACH FRAME $\boldsymbol{t}$

Contact area proportion (CA_[sensing area])			
ID	Parameter	Expression	Description
1	$CA\_B(t)$	$\sum_{B\_X(t)} n(i,j) / N$	Where $n(i,j) = 1$ if the sensor element at position (i,j) is occupied, 0 otherwise. $N = 44 \times 42$
2	$CA\_S(t)$	$\sum_{S\_X(t)} n(i,j) / N$	

Centre Of Pressure (COP_[sensing area]_[direction (Medial-Lateral/Up-Down/Anterior-Posterior)])			
ID	Parameter	Sensing area	Description
3	$COP\_B\_ML(t)$	B_X	The COP of a (combined) sensing area in one specific direction. The value is divided by the corresponding dimension of the (combined) sensing area for normalization.
4	$COP\_B\_UD(t)$	B_X	
5	$COP\_S\_AP(t)$	S_X	
6	$COP\_S\_ML(t)$	S_X	
7	$COP\_SR\_AP(t)$	$S\_X\_R\_X$	
8	$COP\_SL\_AP(t)$	$S\_X\_L\_X$	
9	$COP\_SAL\_ML(t)$	$S\_A\_L\_X$	
10	$COP\_SAR\_ML(t)$	$S\_A\_R\_X$	

Pressure Ratio (PR_[Sensing area 1]_[sensing area 2])				
ID	Parameter	Sensing area 1	Sensing area 2	Description
11	$PR\_BRE\_B(t)$	$B\_X\_R\_E$	B_X	The ratio between the sums of pressure from two (combined) sensing areas.
12	$PR\_BRI\_B(t)$	$B\_X\_R\_I$	B_X	
13	$PR\_BLE\_B(t)$	$B\_X\_L\_E$	B_X	
14	$PR\_BLI\_B(t)$	$B\_X\_L\_I$	B_X	
15	$PR\_BU\_B(t)$	B_U_X	B_X	
16	$PR\_BM\_B(t)$	B_M_X	B_X	
17	$PR\_BD\_B(t)$	B_D_X	B_X	
18	$PR\_SAL\_SL(t)$	$S\_A\_L\_X$	$S\_X\_L\_X$	
19	$PR\_SAR\_SR(t)$	$S\_A\_R\_X$	$S\_X\_R\_X$	
20	$PR\_SLE\_SL(t)$	$S\_X\_L\_E$	$S\_X\_L\_X$	
21	$PR\_SRE\_SR(t)$	$S\_X\_R\_E$	$S\_X\_R\_X$	
22	$PR\_SR\_S(t)$	$S\_X\_R\_X$	S_X	
23	$PR\_SA\_S(t)$	S_A_X	S_X	
24	$PR\_SAR\_SA(t)$	$S\_A\_R\_X$	S_A_X	

Notes. X in the name of a sensing area stands for all possible options in the corresponding code position or thereafter, i.e., S_F_L_X represents the front left part of the seat pan including S_F_L_E and S_F_L_I, while B_X denotes the whole part of backrest. In the parameter name, the X is omitted for brevity.